



Shielding Analysis for the ITER Divertor and Vacuum Pumping Ducts

M.E. Sawan, Y. Gohar, R. Santoro

June 1994

UWFDM-964

Presented at the 3rd International Symposium on Fusion Nuclear Technology, June 26 – July 1, 1994, Los Angeles CA; to be published in *Fusion Engineering and Design*.

FUSION TECHNOLOGY INSTITUTE

UNIVERSITY OF WISCONSIN

MADISON WISCONSIN

DISCLAIMER

This report was prepared as an account of work sponsored by an agency of the United States Government. Neither the United States Government, nor any agency thereof, nor any of their employees, makes any warranty, express or implied, or assumes any legal liability or responsibility for the accuracy, completeness, or usefulness of any information, apparatus, product, or process disclosed, or represents that its use would not infringe privately owned rights. Reference herein to any specific commercial product, process, or service by trade name, trademark, manufacturer, or otherwise, does not necessarily constitute or imply its endorsement, recommendation, or favoring by the United States Government or any agency thereof. The views and opinions of authors expressed herein do not necessarily state or reflect those of the United States Government or any agency thereof.

Shielding Analysis for the ITER Divertor and Vacuum Pumping Ducts

M. E. Sawan

Fusion Technology Institute
University of Wisconsin-Madison
1500 Johnson Drive
Madison, Wisconsin 53706, U.S.A.

Y. Gohar and R. Santoro

ITER Garching Joint Work Site
Max-Planck-Institut für Plasmaphysik
D-85748 Garching bei München, Germany

June 1994

UWFDM-964

Presented at the 3rd International Symposium on Fusion Nuclear Technology, June 26-July 1, 1994, Los Angeles, CA; to be published in *Fusion Engineering and Design*.

Abstract

Three-dimensional shielding analysis has been performed for the ITER outline design presented to TAC-4 in January 1994. The average neutron wall loading in ITER is 0.913 MW/m² for the nominal 1500 MW fusion power. The peak outboard and inboard neutron wall loadings are 1.193 and 0.923 MW/m², respectively. The divertor modules along with the vacuum vessel provide adequate shielding for the TF coils in the divertor region. The walls of the horizontal divertor ducts are completely out of the direct line of sight of source neutrons. The contribution to total nuclear heating from streaming into the 24 divertor ducts is only 0.21 kW without additional duct shielding. No separate divertor duct shielding is needed and the 20 cm thick duct wall along with the 11 cm thick mechanical structure will provide adequate protection for the TF coils against streaming radiation. The values of total nuclear heating in the TF coils are only 4.14 and 4.79 kW for the SS/water blanket-shield and Li/V breeding-blanket designs, respectively.

1. Introduction

The first formal phase of the International Thermonuclear Experimental Reactor (ITER) project was the Conceptual Design Activity (CDA) which was conducted from May 1988 until December 1990 [1]. The ITER project embarked on a new phase called the Engineering Design Activity (EDA) which started in July 1992. An outline design for ITER has been developed during the first eighteen months of the ITER EDA [2]. The design provides a nominal fusion power of 1.5 GW from a single null plasma. Twenty-four toroidal field (TF) coils are employed. A vertical cross section of the design is given in Fig. 1. The design incorporates an advanced divertor concept at the bottom of the reactor. The vacuum vessel (VV) is a double wall structure that acts as a shielding component and containment structure. 24 large lower ports are utilized for assembly and disassembly of the divertor cassettes and for vacuum pumping. Radiation streaming into these ports can produce excessive heating and damage the TF coils in the divertor region. Reducing nuclear heating in the TF coils to acceptable levels particularly in the regions behind the divertor and adjacent to the divertor vacuum pumping ducts has been identified as an important shielding issue.

In this paper, the poloidal distribution of the neutron wall loading in the different regions of ITER is determined using the Monte Carlo code MCNP [3]. The detailed geometrical configuration of the ITER first wall is modeled in the calculation and the source neutrons are sampled from the plasma zone according to the fusion power density distribution within the plasma. Due to the geometrical complexity of the divertor region, three-dimensional analyses are required. The peak magnet radiation effects as well as the integrated nuclear heating have been calculated in the parts of the coils adjacent to the vacuum pumping ducts using MCNP. The total nuclear heating in the TF coils of ITER has been determined taking into account the poloidal variation of the neutron wall loading as well as the poloidal variation of the blanket/shield/vacuum vessel thickness. The total nuclear heating in the TF coils has been calculated for both the nonbreeding 316SS/water blanket-shield and the Li/V breeding-blanket designs.

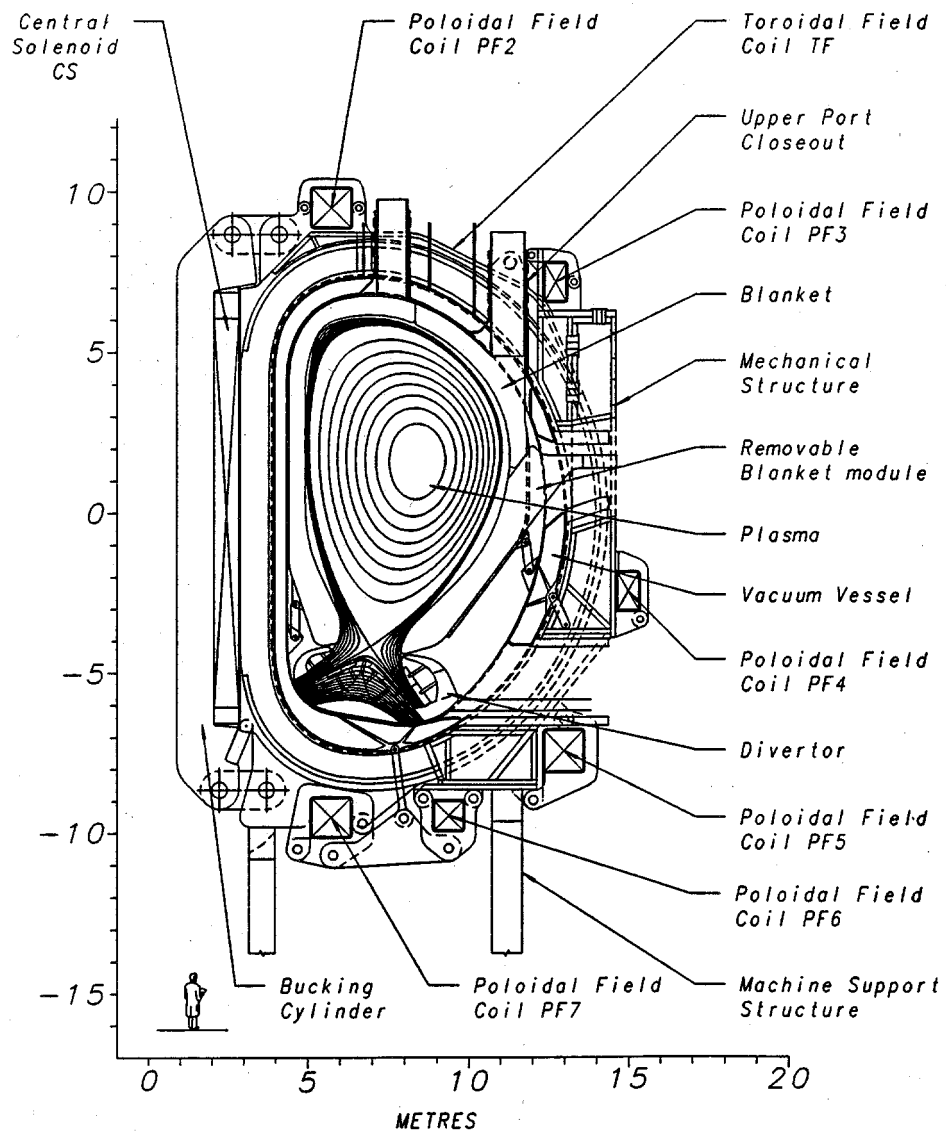


Fig. 1. Vertical cross section of ITER.

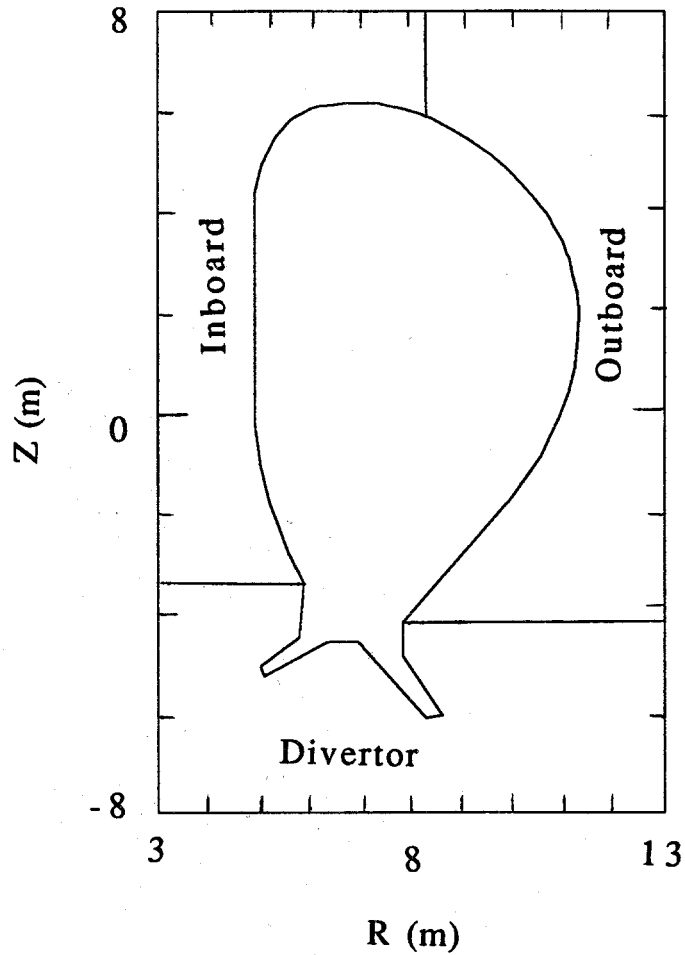


Fig. 2. The ITER first wall geometrical model used in the MCNP calculations.

2. Neutron Wall Loading Distribution

The poloidal distribution of the neutron wall loading in the different regions of ITER has been determined using the three-dimensional radiation transport Monte Carlo code MCNP [3]. The results are normalized to the nominal fusion power of 1500 MW. The detailed geometrical configuration of the ITER first wall has been modeled in the calculation. An output of the MCNP geometry plotting routine is given in Fig. 2. It shows a vertical cross section of the geometrical model used in the calculations. A combination of cones, tori, and cylinders was utilized for accurate modeling of the first wall. Source neutrons are sampled from the plasma zone according to the source distribution within the single null plasma shape. The radial and vertical shifts of the magnetic axis where the fusion power density peaks have been taken into

account. The magnetic axis is located at a radius of 8.633 m and is 1.622 m above the reactor midplane. The direction of source particles has been sampled from an isotropic angular distribution. Three million source particles have been sampled in the MCNP calculation yielding statistical uncertainty less than 0.5 % in the calculated wall loading at any first wall segment.

Source particles travel through void in the plasma chamber until they cross the wall. Particles are killed upon crossing the wall to account for the shadowing effect. Surface current tallies have been determined by counting particles crossing the wall. These current tallies represent the neutron wall loading. In order to get the detailed poloidal distribution of the neutron wall loading, the first wall surface has been segmented into 106 poloidal segments and particles crossing each segment have been tallied. The outboard and inboard first wall surface areas are 800 and 421 m², respectively, and the area at the entrance to the divertor region is 94 m². Therefore, the average neutron wall loading is 0.913 MW/m² for the nominal 1500 MW fusion power. The calculated average neutron wall loadings at the outboard first wall, inboard first wall, and entrance to divertor region are 1.044, 0.735, and 0.6 MW/m², respectively. The total area of surfaces exposed to the plasma in the divertor region is 372 m² with an average neutron wall loading of 0.148 MW/m².

Fig. 3 gives the poloidal variation of neutron wall loading in the outboard and inboard regions as a function of toroidal length measured in the anticlockwise direction from the lower corner of the outboard first wall (point A in Fig. 2). The peak outboard and inboard neutron wall loadings are 1.193 and 0.923 MW/m², respectively. It is clear that the neutron wall loading peaks at vertical locations close to that of the plasma magnetic axis. Fig. 4 shows the poloidal variation of neutron wall loading in the divertor region as a function of length measured in the anticlockwise direction from the upper left corner of the divertor region (point B in Fig. 2). The peak neutron wall loading in the divertor region is 0.559 MW/m² at the upper surface of the middle divertor plate facing the plasma x-point. No direct source neutrons impinge on the inner surface of the inner divertor leg. The average neutron wall loading at the inner surface of the outer divertor leg is only 0.016 MW/m². The values of neutron wall loading at the inner and

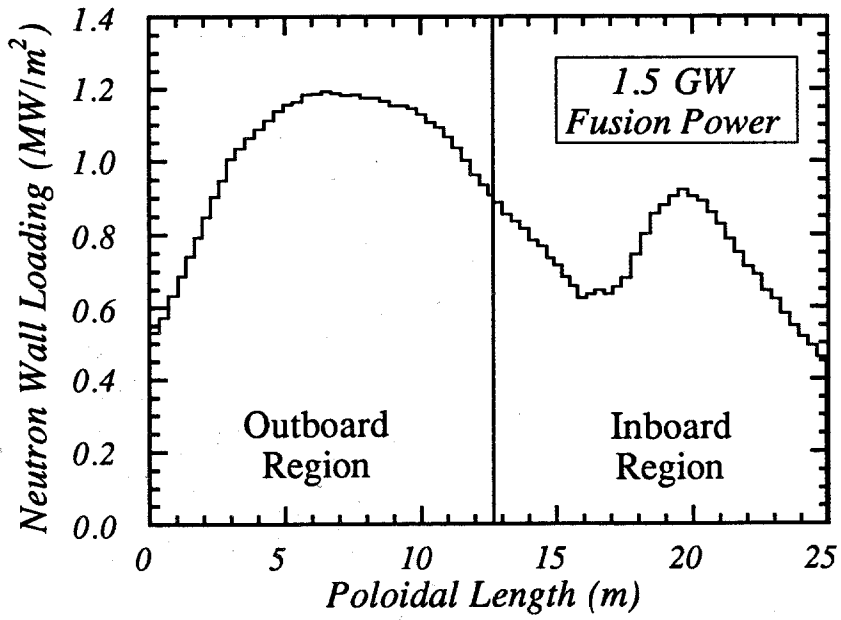


Fig. 3. The poloidal variation of neutron wall loading in the outboard and inboard regions as a function of toroidal length.

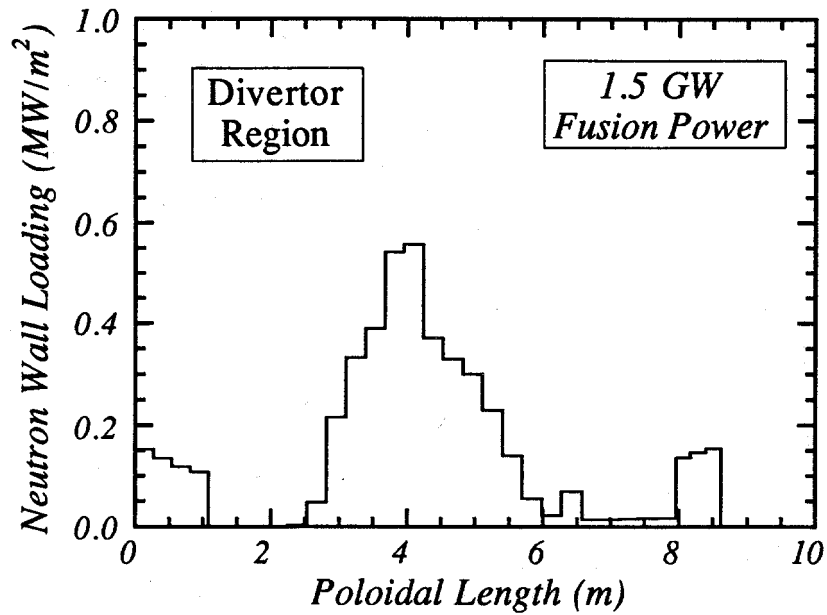


Fig. 4. The poloidal variation of neutron wall loading in the divertor regions as a function of toroidal length.

outer divertor dump plates with the least magnet shielding space are 0.0009 and 0.07 MW/m², respectively. These results are for the nominal 1500 MW fusion power. During the plasma power excursions of 1800 MW fusion power, these values will be 20% higher.

3. Three-Dimensional Shielding Model

Providing adequate protection for the TF coils against radiation streaming into the divertor vacuum pumping ducts has been identified as an important shielding issue for the current ITER design. Due to the geometrical complexity of the divertor region, three-dimensional models are required to properly determine the radiation effects in the parts of the TF coils adjacent to the divertor vacuum pumping duct. Furthermore, the parts of the TF coils behind the divertor are protected from source neutrons by the divertor modules and the vacuum vessel with varying thickness and geometrical shape. Magnet hot spots are expected behind the inner and outer divertor dump plates where the shielding space is minimal. At these locations the combined thickness of the divertor and vacuum vessel is only about 90 cm. Again, three-dimensional calculations are needed to determine magnet damage in these zones.

Three-dimensional neutron-gamma transport calculations have started for magnet shielding in the divertor region taking into account streaming into the divertor vacuum pumping ducts. The continuous energy, coupled neutron-gamma-ray Monte Carlo code MCNP [3] has been used. The nuclear data used is based on the ENDF/B-V evaluation. A three-dimensional model has been developed for the ITER reactor to be used with the MCNP code. The model developed here is based on the present ITER outline design [2] and will need additional modifications in the future as the ITER design evolves and more detailed geometrical aspects of the design become available.

The detailed geometrical configuration of the first wall, blanket, shield, vacuum vessel, divertor and TF coils in the current ITER design has been modeled in the calculation. Several additional surfaces have been added in the divertor region to allow for utilizing the geometry splitting with Russian Roulette variance reduction techniques employed in MCNP. Due to

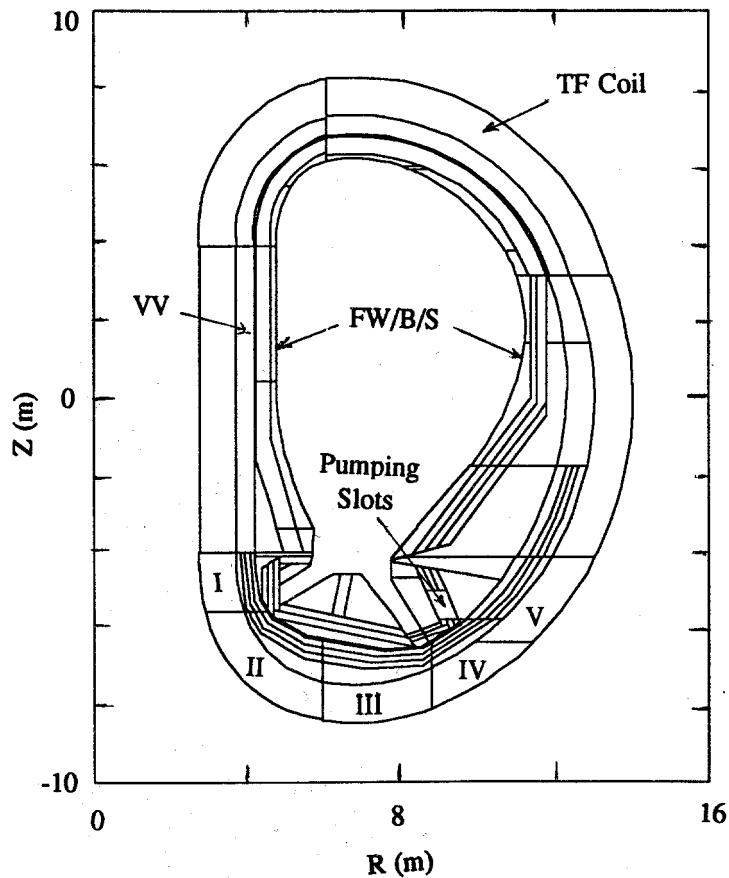


Fig. 5. A vertical cross section through the middle of the TF coil.

symmetry, only 1/48 of the reactor is modeled with surrounding reflecting boundaries. The model includes half a TF coil and half a divertor duct. The toroidal angle for the model used is 7.5 degrees.

The output of the MCNP geometry plotting routine given in Fig. 5 shows a vertical cross section through the middle of the TF coil. This cross section cuts through one of the pumping slots in the outer leg of the divertor. There are five such slots in each of the 24 divertor modules. The TF magnet in the divertor region is divided into five zones as indicated in Fig. 5. The first zone is behind the inner divertor dump plate, the second zone is behind the inner part of the divertor, the third zone is behind the outer part of the divertor, the fourth zone is behind the outer divertor dump plate, and the fifth zone is adjacent to the divertor vacuum pumping duct. A vertical cross section through the center of the divertor duct is shown in Fig. 6. Fig. 7 is a

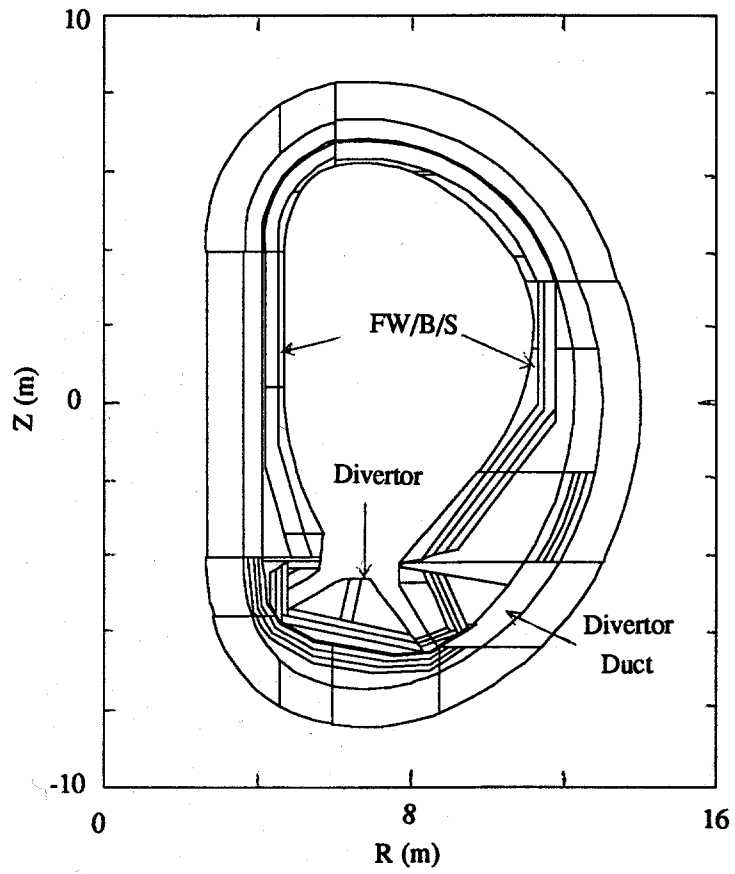


Fig. 6. A vertical cross section through the center of the divertor duct.

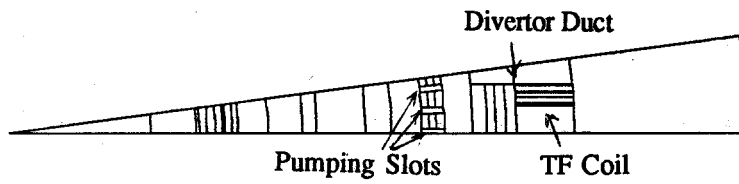


Fig. 7. A horizontal cross section at the middle of the divertor vacuum pumping duct.

horizontal cross section at $z = -5.5$ m in the middle of the divertor vacuum pumping duct. The divertor pumping slots in the outer leg of the divertor are shown in this figure. Also shown are the shielding layers between the duct and the coil consisting of the 3 cm thick front Inconel wall, the 14 cm thick steel/water zone, and the 3 cm thick back Inconel wall of the duct wall as well as the 11 cm thick mechanical structure.

A combination of cones, tori, cylinders, and planes was utilized for accurate modeling of the geometry. A total of 147 surfaces has been used in the model, of which 32 are fourth degree tori and 58 are cones. The model employs 119 geometrical cells. The volumes of the different cells and the areas of surfaces of interest have been determined stochastically by ray tracing. In this calculation, all cells are assumed to not include any material and the geometrical model has been sprayed by 10 million particles at random directions. This calculation serves also as a mean for geometry checking by making sure that each point in space belongs to one of the cells used in the model. This calculation provided a successful check for the geometrical model.

The MCNP code has been modified to sample source neutrons from the plasma zone according to the source distribution, provided by the ITER JCT team, with the single null plasma shape as explained in the previous section. Source neutrons are biased to improve the statistical uncertainty in the calculated magnet responses in the divertor region. Surface flux tallies are used to determine the radiation effects at the front and side surfaces of the TF coils in the divertor region and cell energy deposition tallies are used to determine the total magnet heating in the five magnet zones used in the divertor region.

In this calculation, it is assumed that no additional divertor duct shielding is utilized and magnet protection is provided by the 20 cm thick duct wall along with the 11 cm thick mechanical structure. No credit is taken for the additional shielding provided by the divertor coolant supply lines inside the duct. In addition, no credit is taken for the fins and support structure at the inner surfaces of the divertor legs that provide additional radiation attenuation. However, the model developed for MCNP calculations includes cells representing the zones where these fins and their support structure can be included. Although this calculation assumes

void in these cells, structural material with the appropriate density factor can be used in these cells in the future to assess the impact on magnet shielding. Different material compositions are assumed for the different cells used in the model. The blanket is assumed to consist of 70% 316 SS and 30% water. The vacuum vessel composition used includes 12% Inconel 625, 55% 316 SS and 33% water. The filling material for the duct wall is 60% 316 SS and 40% water. The mechanical structure at the sides of the magnets is made of 316 SS and the divertor module consists of 70% 316 SS and 30% water. The TF coil composition used in the calculation is 31.6% SS, 26% Cu, 9.5% non-Cu (2.5% Nb₃Sn, 6.4% Bronze, 0.6% V), 21.1% liquid He, and 11.8% insulator (epoxy with 70% R-glass).

The calculation has been performed using 200,000 source particles yielding statistical uncertainties less than 10% in the calculated magnet nuclear responses at the locations of interest. The results are normalized to the nominal fusion power of 1500 MW. The end of life fluence related radiation effects have been determined for 3 full power years (FPY) of operation.

4. Magnet Radiation Effects in the Divertor Region

Table 1 gives the magnet radiation effects in the part of the TF coil adjacent to the divertor vacuum pumping duct (zone V in Fig. 5). The results are given at the front and side surfaces of the coil. It is clear that the sides of the TF coils are well protected from radiation streaming into the divertor vacuum pumping ducts. The contribution to total magnet heating from the parts of the coils adjacent to the divertor ducts is only 0.21 kW.

Table 2 gives the magnet radiation effects averaged over the front surface of the TF coil in zones I, II, III, and IV shown in Fig. 5. The largest magnet radiation effects are in zone IV behind the outer divertor dump plates where the shielding space is minimal. Although the shielding space behind the inner divertor dump plates is smaller, the magnet radiation effects in zone I are lower than those in zone IV since the inner divertor dump plates have a direct view of a smaller part of the plasma with lower power density. The values of neutron wall loading at the

Table 1. Magnet Radiation Effects at the Front and Side Surfaces of the TF Coils Adjacent to the Divertor Duct

	Front Surface	Side Surface
End-of-Life Organic Insulator Dose (Rads @ 3 FPY)	1.50×10^7	3.53×10^7
End-of Life Fast Neutron Fluence in Magnet (n/cm ² @ 3 FPY)	8.22×10^{15}	4.14×10^{16}
End-of-Life Cu dpa in Magnet (dpa @ 3 FPY)	4.11×10^{-6}	1.82×10^{-5}
Specific Nuclear Heating in Magnet (mW/cm ³)	0.0084	0.014

Table 2. Magnet Radiation Effects at the Front Surface of the TF Coil Behind the Divertor

Zone	I	II	III	IV
End-of-Life Organic Insulator Dose (Rads @ 3 FPY)	1.69×10^7	2.44×10^6	1.62×10^6	4.04×10^7
End-of Life Fast Neutron Fluence in Magnet (n/cm ² @ 3 FPY)	7.11×10^{15}	9.93×10^{15}	5.10×10^{14}	2.90×10^{16}
End-of-Life Cu dpa in Magnet (dpa @ 3 FPY)	7.83×10^{-6}	7.26×10^{-7}	2.31×10^{-7}	1.82×10^{-5}
Specific Nuclear Heating in Magnet (mW/cm ³)	0.0081	0.0047	0.0011	0.018

inner and outer divertor dump plates are 0.0009 and 0.07 MW/m², respectively. It should be noted that the radiation effects in the magnet zones I to IV calculated here are conservative since no credit is taken for attenuation in the divertor fins and their support structure, the mechanical structure at the sides of the coils, and the lower wall of the divertor duct. The calculated radiation effects are much lower than the radiation limits considered in ITER.

5. Total Nuclear Heating in the TF Coils

The contribution to total magnet heating from the parts of the coils in the divertor region are 0.034, 0.0063, 0.046, 0.87, and 0.21 kW, in zones I, II, III, IV, and V, respectively. The total heating in the 24 TF coils contributed by the divertor region is 1.17 kW. The parts of the TF coils behind the divertor are protected from source neutrons by the divertor modules and the vacuum vessel. The smallest shielding space is behind the inner and outer divertor dump plates as shown in Fig. 5. At these locations the combined thickness of the divertor and vacuum vessel is 96 cm. The thickness increases rapidly as one moves away from the dump plates reaching 250 cm at the middle of the divertor where the neutron wall loading peaks at 0.56 MW/m^2 . Hence, magnet heating behind the divertor is dominated by heating in the areas behind the divertor dump plates. Nuclear heating in the parts of the magnets adjacent to the divertor vacuum pumping ducts has been determined to be only 0.21 kW. This assumes that no separate duct shield is used.

The parts of the TF coils behind the upper and the middle straight segments of the inboard blanket have a combined blanket/shield/vacuum vessel thickness of 100 cm between them and the plasma and an average neutron wall loading of 0.783 MW/m^2 . One-dimensional calculations have been performed for these sections to determine the nuclear heating per meter length of the TF coils. The calculations have been performed using the discrete ordinates code ONEDANT [4] for both the nonbreeding 316SS/water blanket-shield and the Li/V breeding-blanket designs. For 1 MW/m^2 neutron wall loading, the results are 0.196 and 0.239 kW/m for the SS/water and Li/V options, respectively. Based on these results the values for total magnet heating in the parts of the TF coils behind the upper and the middle straight segments of the inboard blanket are 1.26 and 1.53 kW for the SS/water and Li/V options, respectively. The lower curved portion of the inboard blanket increases in thickness as one moves towards the lower tip of it as shown in Fig. 1. In addition, the neutron wall loading drops from 0.83 MW/m^2 at the upper end of this blanket segment to 0.46 MW/m^2 at the lower tip. An appropriate integration procedure, that takes into account the variation of both the neutron wall loading and the blanket/shield/vacuum

Table 3. Total Nuclear Heating (kW) in the TF Coils of ITER

	316SS/Water Blanket-Shield	Li/V Breeding-Blanket
Inboard Region	1.34	1.63
Outboard Region	1.63	1.99
Divertor Region	1.17	1.17
Total	4.14	4.79

vessel thickness, has been utilized to determine nuclear heating in the parts of the TF coils behind this blanket segment. This yields 0.08 and 0.1 kW for the SS/water and Li/V options, respectively.

The parts of the TF coils behind the upper segment of the outboard blanket have a combined blanket/shield/vacuum vessel thickness of 100 cm between them and the plasma and an average neutron wall loading of 1.141 MW/m². The values for total magnet heating in these parts of the TF coils have been determined to be 1.33 and 1.63 kW for the SS/water and Li/V options, respectively. The lower segment of the outboard blanket as well as the part of the vacuum vessel behind it increase in thickness as one moves towards the lower tip of it as shown in Fig. 1. In addition, the neutron wall loading drops from 1.193 MW/m² at the upper end of this blanket segment to 0.531 MW/m² at the lower tip. An integration procedure was utilized yielding 0.3 and 0.36 kW for the SS/water and Li/V options, respectively. Table 3 gives the magnet nuclear heating in the different reactor regions for both the nonbreeding 316SS/water blanket-shield and the Li/V breeding-blanket designs. The values for the total nuclear heating in the 24 TF coils are 4.14 and 4.79 kW for the SS/water and Li/V options, respectively. All these values do not include any safety factor.

6. Summary and Conclusions

The poloidal distribution of the neutron wall loading in the different regions of ITER has been determined using the Monte Carlo code MCNP. The average neutron wall loading is 0.913 MW/m² for the nominal 1500 MW fusion power. The calculated average neutron wall loadings at the outboard and inboard first walls, are 1.044 and 0.735 MW/m², respectively. The peak outboard and inboard neutron wall loadings are 1.193 and 0.923 MW/m², respectively.

The walls of the horizontal ducts are completely out of the direct line of sight of source neutrons. The ducts are shielded from the plasma region by the approximately 80 cm thick lower end of the outboard blanket/shield and by the 40-60 cm thick outer divertor leg in front of the lower half of the duct. The contribution to total nuclear heating from streaming into the 24 divertor ducts is only 0.21 kW without additional duct shielding. Based on this analysis, it is concluded that no additional divertor duct shielding will be needed and the 20 cm thick duct wall along with the 11 cm thick mechanical structure will provide adequate protection for the TF coils against streaming radiation.

The total nuclear heating in the TF coils of ITER has been determined taking into account the poloidal variation of the neutron wall loading as well as the poloidal variation of the blanket/shield/vacuum vessel thickness. The values of total nuclear heating in the TF coils are 4.14 and 4.79 kW for the SS/water blanket-shield and Li/V breeding-blanket designs, respectively. These values are lower than the nuclear heating limit of ~10 kW for the TF coils.

Acknowledgment

Support for this work was provided by the U.S. Department of Energy.

References

- [1] ITER Conceptual Design Report, ITER Documentation Series no. 18, IAEA, Vienna, 1991.
- [2] P-H. Rebut, Detail of the ITER outline design report, ITER Report, ITER-TAC-4-06, Vols. 1-3, 10 January 1994.
- [3] J. Briesmeister (Editor), MCNP, a general Monte Carlo code for neutron and photon transport, version 3A, LA-7396-M, Rev. 2, Los Alamos National Laboratory (September 1986, revised April 1991) and Summary of MCNP Commands, Version 4.2, LANL Draft (September 1991).
- [4] R.D. O'Dell et al., User's manual for ONEDANT: a code package for one-dimensional, diffusion-accelerated, neutral particle transport, Los Alamos National Laboratory Report, LA-9184-M (1982).